ESKİŞEHİR TECHNICAL UNIVERSITY JOURNAL OF SCIENCE AND TECHNOLOGY
A- APPLIED SCIENCES AND ENGINEERING

2023, 24(1), pp. 57-70, DOI: 10.18038/estubtda.1248808

RESEARCH ARTICLE

# ASYMPTOTIC ANALYSIS OF ACOUSTIC GREEN'S FUNCTIONS

**Hazel YÜCEL [1,*], Yağmur Ece UÇAR [2]**

[1] Department of Computer Engineering, Başkent University, Ankara, Turkey
[2] Department of Mathematics, Eskişehir Technical University, Eskişehir, Turkey

## ABSTRACT

An asymptotic expansion of layered Green's function is examination in a spatial domain and parametric approach is proposed by determining a small parameter to derive the shortened form of Green's function for 3- and 4-layered structures. For qualitative testing and comparison of the exact Green's function and asymptotic shortened Green's functions associated with the measurement and source point in the same layer, we performed numerical calculations.

**Keywords:** Green's function, Layered media, Parametric analysis, Asymptotic approach

## 1. INTRODUCTION

In acoustic imaging, the measured waves are converted to image using certain algorithms commonly involving the Green's functions [1,3]. Considering the layered acoustic environment, which includes different acoustical and physical parameters, the layered Green's functions involving infinite integrals with highly oscillatory and slowly attenuating integrands must be calculated. [4,5]. In [6], an out-of-plane analysis of a layered elastic plate using asymptotic expansions are investigated whereas low-frequency analysis of multi-component rods are considered employing an asymptotic procedure together with a multiparametric analysis of the problem parameters in [7]. In both works, approximate analytical solutions were obtained and dispersion equations, which are difficult or impossible to calculate analytically due to the complicated functions they contain, are expressed through simplified polynomials resulting in much simpler analysis of the considered problems. In [8] a parametric analysis was performed to evaluate the effect of layer densities on the Green's function.

It is therefore possible to formulate the mathematical model of the problem considered in this paper through the physical and acoustic parameters in an understandable way whereby a multiparametric approach may be utilized after a successful application of an asymptotic expansion to the layered Green's function in a spatial domain [9].

In this study, asymptotic expansions of each term in the coefficients of acoustic layer Green's functions used in the solution of the photoacoustic wave equation are obtained for 3 and 4 layers in spatial domain, and a parametric analysis is carried out according to medium velocities for a 3 layered media. Numerical comparisons of exact Green's functions and Green's functions obtained through the asymptotic expansions of coefficients are given. Using these expansions in photoacoustic imaging can both provide a physical interpretation of the problem and speed up the calculation time.

*Corresponding Author: hazelyucel@gmail.com
Received: 01.12.2022 Published: 29.03.2023

## 2. STATEMENT OF THE PROBLEM

The medium is modeled as a layered planar medium consisting of 3 and 4 layers, respectively, each of which is homogeneous with different acoustic properties from others, extending infinitely in the transverse direction, subject to continuity conditions on the boundary of layers and the wave propagation is represented by layered Green's functions.

Assuming that the source and measurement locations are in the same layer, $r = (x, z)$ and $r' = (x', z')$, respectively, acoustic layered Green's functions are expressed as follows [8]:

$$G(r, r') = \int_0^\infty \frac{\cos\big(k_x(x - x')\big)}{k_{z1}} \left(e^{(-k_{z1}|z-z'|)} + R_N e^{(-k_{z1}|z+z'|)}\right) dk_x \qquad N = 3{,}4 \qquad (1)$$

where $R_N$ denotes transmission and reflection coefficients. Equations $k_x^2 = k_{zi}^2 + k_i^2$ are valid and the variables of this equations are wave numbers ($i = 1, 2, 3, 4.$).

The initial condition at $t = 0$, and continuity conditions on the boundary are expressed as

$$p_0 = p(r, t = 0), \qquad \frac{\partial p(r, t = 0)}{\partial t} = 0 \qquad (2)$$

$$\lim_{r \to S_m^-} p(r, t) = \lim_{r \to S_m^+} p(r, t) \qquad (3)$$

and

$$\lim_{r \to S_m^-} \frac{1}{\rho_m} \frac{\partial p(r, t)}{\partial \mathbf{n}} = \lim_{r \to S_m^+} \frac{1}{\rho_{m+1}} \frac{\partial p(r, t)}{\partial \mathbf{n}}. \qquad m = 1{,}2{,}3{,}4 \qquad (4)$$

Here, $p(r, t)$ is the acoustic wave function at position $r$ and time $t$. $S_m$ denotes the surface of the $m^{th}$ boundary. $\rho_m$ and $\rho_{m+1}$ are densities of the layers $m$ and $m + 1$, respectively. Also, since the geometry of the problem is taken as unbounded from above and below, thus, radiation conditions are valid at infinity.

To simplify the analysis, we introduce a dimensionless spatial wave number $K_x$, and the spectral frequency $\Omega$ given by

$$\Omega = \frac{\omega\, h_2}{c_1}, \qquad K_x = k_x\, h_2\,, \qquad (5)$$

where $h_2$ is the thickness between the first and second layers. We introduce the dimensionless acoustic velocity and density ratios as

$$\chi_{1m} = \frac{c_1}{c_m}, \qquad \rho_{nm} = \frac{\rho_n}{\rho_m}, \qquad m = 2{,}3{,}4;\ n = m - 1. \qquad (6)$$

Using non-dimensional parameters, the wave numbers appearing in eqn.(1) are rewritten as

$$K_{z_1} = \begin{cases} -i\sqrt{\Omega^2 - K_x^2}, & |\Omega| > |K_x| \\ \sqrt{K_x^2 - \Omega^2}, & |K_x| > |\Omega| \end{cases}, \qquad (7)$$

$$K_{z_m} = \begin{cases} -i\sqrt{\Omega^2 \chi_{1m}^2 - K_x^2}, & |\Omega \chi_{1m}| > |K_x| \\ \sqrt{K_x^2 - \chi_{1m}^2 \Omega^2}, & |K_x| > |\chi_{1m} \Omega| \end{cases}, \qquad m = 2, 3, 4. \qquad (8)$$

## 2.1. 3- LAYERED MEDIA

For a 3 layer media, the geometry of problem is given in following figure.

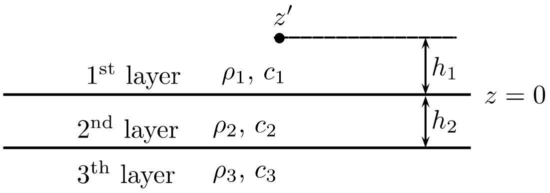


**Figure 1**. Geometry of 3-layer media.

Here, $\rho_i$ and $c_i$ are the density and velocity of medium, respectively ($i = 1, 2, 3$). $h_1$ is the distance between the source and first layer, $h_2$ is the thickness between layers and the source is located the first layer at $z'$. The Green's function, in this case, takes the form

$$G_1 = \frac{1}{2\pi}\int_0^{\infty}\left(e^{-k_{z_1}|z-z'|} + R_3 e^{-k_{z_1}|z+z'|}\right)\frac{cos\left(k_x(x-x')\right)}{k_{z_1}}dk_x, \qquad z\epsilon \text{ Medium 1.} \tag{9}$$

The coefficients $R_3$ can be written as a piecewise function for the first, second and third regions of integration, as $K_x < \Omega$, $\Omega - \varepsilon < K_x < \Omega + \varepsilon$ and $K_x > \Omega$ , respectively. For these regions, the coefficient of layered Green's function is represented as

$$R_3 = \begin{cases} R_3^{(I)}, & K_x < \Omega \\ R_3^{(II)}, & K_x\,\epsilon(\Omega - \varepsilon, \Omega + \varepsilon), \\ R_3^{(III)}, & \Omega < K_x \end{cases} \tag{10}$$

$$R_3 = \frac{E_3}{\Delta_3}, \tag{11}$$

where $E_3$ and $\Delta_3$ are calculated using boundary conditions on the interfaces of layers which includes the physical and acoustic parameters of the medium. The coefficient of Green's function given in equation (10) may be expanded in the small variables, $\frac{K_x}{\Omega} \ll 1$ and $\frac{\Omega}{K_x} \ll 1$, in the 1st and 3rd regions, respectively. At the branch points, the coefficient of $R_3^{(II)}$ is calculated numerically since an asymptotic expansion around these points is not visible.

When the source and measurement points are located in the first layer as depicted in Figure 1, the coefficient ($R_3$) of the Green's function is given by

$$\frac{E_3}{\Delta_3} = \frac{-\cosh\left(K_{z_2}\right)K_{z_2}\left(\rho_{13}K_{z_3} + K_{z_1}\right) + \sinh\left(K_{z_2}\right)\left(\rho_{23}K_{z_1}K_{z_3} + \rho_{12}K_{z_2}^{\,2}\right)}{\cosh\left(K_{z_2}\right)K_{z_2}\left(\rho_{13}K_{z_3} - K_{z_1}\right) + \sinh\left(K_{z_2}\right)\left(\rho_{23}K_{z_1}K_{z_3} - \rho_{12}K_{z_2}^{\,2}\right)}. \tag{12}$$

On expanding each term of the ratio $\frac{E_3}{\Delta_3}$ in an asymptotic series, equation (12) maybe reduced to a polynomial. As an example, the series expansions of the following two terms are given in the first region:

$$\cosh\left(K_{z_2}\right) = 1 + \frac{K_{z_2}^{\,2}}{2!} + \cdots = 1 + \frac{K_x^2 - \Omega^2}{2} + \cdots = \Omega^2\left(\frac{1}{\Omega^2} + \frac{K_x^2}{2\Omega^2} - \frac{1}{2}\right) + O\left(\frac{K_x^4}{\Omega^4}\right), \tag{13}$$

$$K_{z_3} = \sqrt{K_x^2 - \chi_{13}^2\Omega^2} = i\chi_{13}\Omega\sqrt{1 - \frac{K_x^2}{\chi_{13}^2\Omega^2}} = i\chi_{13}\Omega\left(1 - \frac{K_x^2}{2\chi_{13}^2\Omega^2} + O\left(\frac{K_x^4}{\Omega^4}\right)\right). \tag{14}$$

Assuming $\Omega \gg 1$, asymptotic order of each term in (12) can be decided on expanding the expression $\frac{a\Omega+b}{c\Omega+d}$ where the constants $a, b, c$ and $d$ can be easily determined from (12).

**Case 1:**

In this case, asymptotic expansion of all terms of the coefficient of the Green's function is carried out by assuming that $\frac{K_x}{\Omega} \ll 1$.

If the asymptotic expressions of all terms contained in the coefficient of Green's function given by equation (12) are written, similar to the equations (13) and (14), the first two terms of the numerator $E_3$ and denominator $\Delta_3$ are obtained for the first region ($\Omega \gg K_x$), respectively as follows:

$$\begin{aligned} E_{3(1^{st}region)} \sim & -i\rho_{13}\chi_{13}\Omega^5\frac{\chi_{12}^4}{2} - i\Omega^5\frac{\chi_{12}^4}{2} + \chi_{12}^2\chi_{13}\rho_{23}\Omega^4 + \chi_{12}^4\rho_{12}\Omega^4 \\ & + \frac{K_x^2}{\Omega^2}\left(i\rho_{13}\chi_{13}\Omega^5\left(\chi_{12}^2 + \frac{\chi_{12}^4}{4\chi_{13}^2} - \frac{1}{\Omega^2} - \frac{\chi_{12}^2}{2\Omega^2}\right)\right. \\ & + i\Omega^5\left(\frac{\chi_{12}^2}{4} + \frac{\chi_{12}^4}{4} - \frac{1}{\Omega^2} - \frac{\chi_{12}^2}{2\Omega^2}\right) - \chi_{13}\rho_{23}\Omega^4\left(1 + \frac{\chi_{12}^2}{2\chi_{13}^2} + \frac{\chi_{12}^2}{2}\right) \\ & \left. - 2\rho_{12}\Omega^4\chi_{12}^2\right), \end{aligned} \tag{15}$$

$$\begin{aligned} \Delta_{3(1^{st}region)} \sim & \, i\rho_{13}\chi_{13}\Omega^5\frac{\chi_{12}^4}{2} - i\Omega^5\frac{\chi_{12}^4}{2} + \chi_{12}^2\chi_{13}\rho_{23}\Omega^4 - \chi_{12}^4\rho_{12}\Omega^4 \\ & - \frac{K_x^2}{\Omega^2}\left(i\rho_{13}\chi_{13}\Omega^5\left(\chi_{12}^2 + \frac{\chi_{12}^4}{4\chi_{13}^2} - \frac{1}{\Omega^2} - \frac{\chi_{12}^2}{2\Omega^2}\right)\right. \\ & + i\Omega^5\left(\frac{\chi_{12}^2}{4} + \frac{\chi_{12}^4}{4} - \frac{1}{\Omega^2} - \frac{\chi_{12}^2}{2\Omega^2}\right) - \chi_{13}\rho_{23}\Omega^4\left(1 + \frac{\chi_{12}^2}{2\chi_{13}^2} + \frac{\chi_{12}^2}{2}\right) \\ & \left. + 2\rho_{12}\Omega^4\chi_{12}^2\right). \end{aligned} \tag{16}$$

Substituting equations (15) and (16) in (12), we obtain the coefficient $R_3$ for the fist region as follows

$$R_3^{(I)} = \frac{\Omega^5\left(1+O\left(\frac{K_x^2}{\Omega^2}\right)\right) - \Omega^4\left(1+O\left(\frac{K_x^2}{\Omega^2}\right)\right)}{\Omega^5\left(1+O\left(\frac{K_x^2}{\Omega^2}\right)\right) - \Omega^4\left(1+O\left(\frac{K_x^2}{\Omega^2}\right)\right)}. \tag{17}$$

Since the term $\Omega^5$ is the dominant term in the first region, the coefficient $R_{3(1^{st}\,region)}$ may be written in the shortened form as

$$R_3^{(I)} = \frac{-i\rho_{13}\chi_{13}\Omega^5\frac{\chi_{12}^4}{2} - i\Omega^5\frac{\chi_{12}^4}{2} + \frac{K_x^2}{\Omega^2}\left(i\rho_{13}\chi_{13}\Omega^5\left(\chi_{12}^2 + \frac{\chi_{12}^4}{4\chi_{13}^2} - \frac{1}{\Omega^2} - \frac{\chi_{12}^2}{2\Omega^2}\right) + i\Omega^5\left(\frac{\chi_{12}^2}{4} + \frac{\chi_{12}^4}{4} - \frac{1}{\Omega^2} - \frac{\chi_{12}^2}{2\Omega^2}\right)\right)}{i\rho_{13}\chi_{13}\Omega^5\frac{\chi_{12}^4}{2} - i\Omega^5\frac{\chi_{12}^4}{2} + \frac{K_x^2}{\Omega^2}\left(i\rho_{13}\chi_{13}\Omega^5\left(\chi_{12}^2 + \frac{\chi_{12}^4}{4\chi_{13}^2} - \frac{1}{\Omega^2} - \frac{\chi_{12}^2}{2\Omega^2}\right) + i\Omega^5\left(\frac{\chi_{12}^2}{4} + \frac{\chi_{12}^4}{4} - \frac{1}{\Omega^2} - \frac{\chi_{12}^2}{2\Omega^2}\right)\right)}. \tag{18}$$

Comparisons of exact Green's function and asymptotic Green's function and the relative error are given in the following numerical implementations. In all our computations, we have considered the temporal frequency as 1 MHz and the wavelength as $\lambda = 16x10^{-4}m$. Densities of medium are $\rho_1 = 500\ gr/cm^3, \rho_2 = 700\ gr/cm^3, \rho_3 = 600\ gr/cm^3$ respectively, and veocities of medium are $c_1 = 1600\ m/sec, c_2 = 1000\ m/sec, c_3 = 500\ m/sec$, respectively. Layer thickness is taken as $|h_2| =$

$3\lambda$. The source is located at $(x', z') = (2\lambda, 2\lambda)$ and the measurement point is fixed at $2\lambda$ in the $x$-coordinate but in the $z$-axis the measurement point is varied from $2.001\lambda$ to $11\lambda$.

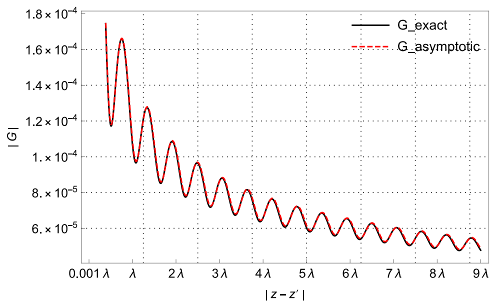


**Figure 2.** Comparison of exact and asymptotic Green's function for a three layered media for the first region

It can be seen from Figure 2, that there is a notable overlap between the absolute value of exact and asymptotic Green's function for all points both in the near and far fields in the first region.

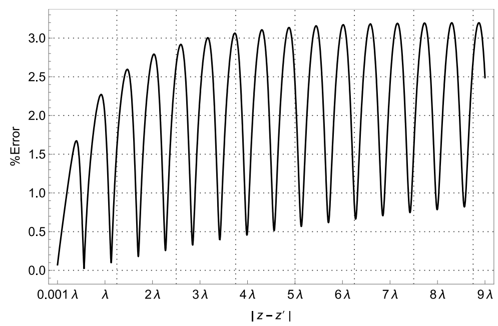


**Figure 3.** Relative error of exact and asymptotic Green's function for a three-layered media for the first region

The relative error, presented in Figure 3, between exact and asymptotic Green's function is limited to about 3% for all distances.

**Case 2:**

By taking $\frac{\Omega}{K_x}$ as the small parameter, similar calculations for $R_3$ can be repeated for the third region giving the numerator $E_3$ and the denominator $\Delta_3$ of coefficients $R_3$ by

$$E_{3(3^{rd}region)} = \left(1 - \frac{\Omega^2}{2\,K_x^2} + \frac{1}{24}\frac{\Omega^4}{K_x^4}\right) - \rho_{13}\left(1 - \frac{\chi_{13}^2}{2}\frac{\Omega^2}{2\,K_x^2} + \frac{\chi_{13}^4}{24}\frac{\Omega^4}{K_x^4}\right) - \rho_{12} + \rho_{23} + \frac{\Omega^2}{K_x^2}\left(\rho_{12}\chi_{12}^2 + \frac{\rho_{23}}{2} + \chi_{13}^2\frac{\rho_{23}}{2}\right) + \frac{\Omega^4}{K_x^4}\left(\frac{\rho_{23}}{24} + \chi_{13}^2\frac{\rho_{23}}{4} + \chi_{13}^4\frac{\rho_{23}}{24}\right), \quad (19)$$

$$\Delta_{3(3^{rd}region)} = \left(1 - \frac{\Omega^2}{2\,K_x^2} + \frac{1}{24}\frac{\Omega^4}{K_x^4}\right) + \rho_{13}\left(1 - \frac{\chi_{13}^2}{2}\frac{\Omega^2}{2\,K_x^2} + \frac{\chi_{13}^4}{24}\frac{\Omega^4}{K_x^4}\right) + \rho_{12} + \rho_{23} + \frac{\Omega^2}{K_x^2}\left(-\rho_{12}\chi_{12}^2 + \frac{\rho_{23}}{2} + \chi_{13}^2\frac{\rho_{23}}{2}\right) + \frac{\Omega^4}{K_x^4}\left(\frac{\rho_{23}}{24} + \chi_{13}^2\frac{\rho_{23}}{4} + \chi_{13}^4\frac{\rho_{23}}{24}\right). \quad (20)$$

The coefficient of Green's function, therefore, takes the form

$$R_3^{(III)} = \frac{\mathrm{K}_\mathrm{x}^5\left(1+O\left(\frac{\Omega^2}{\mathrm{K}_\mathrm{x}^2}\right)\right)+\mathrm{K}_\mathrm{x}^5\left(1+O\left(\frac{\Omega^2}{\mathrm{K}_\mathrm{x}^2}\right)\right)-\mathrm{K}_\mathrm{x}^4\left(1+O\left(\frac{\Omega^2}{\mathrm{K}_\mathrm{x}^2}\right)\right)-K_x^4\left(1+O\left(\frac{\Omega^2}{\mathrm{K}_\mathrm{x}^2}\right)\right)}{\mathrm{K}_\mathrm{x}^5\left(1+O\left(\frac{\Omega^2}{\mathrm{K}_\mathrm{x}^2}\right)\right)-\mathrm{K}_\mathrm{x}^5\left(1+O\left(\frac{\Omega^2}{\mathrm{K}_\mathrm{x}^2}\right)\right)+\mathrm{K}_\mathrm{x}^4\left(1+O\left(\frac{\Omega^2}{\mathrm{K}_\mathrm{x}^2}\right)\right)-\mathrm{K}_\mathrm{x}^4\left(1+\left(\frac{\Omega^2}{\mathrm{K}_\mathrm{x}^2}\right)\right)} \tag{21}$$

Since the variable $K_x$ is much larger than the frequency $\Omega$ in this region, the coefficient $R_3^{(III)}$ can be approximately written as

$$R_3^{(III)} = \frac{\left(1-\frac{\Omega^2}{2\,K_x^2}+\frac{1}{24}\frac{\Omega^4}{K_x^4}\right)-\rho_{13}\left(1-\frac{\chi_{13}^2}{2}\frac{\Omega^2}{2\,K_x^2}+\frac{\chi_{13}^4}{24}\frac{\Omega^4}{K_x^4}\right)}{\left(1-\frac{\Omega^2}{2\,K_x^2}+\frac{1}{24}\frac{\Omega^4}{K_x^4}\right)+\rho_{13}\left(1-\frac{\chi_{13}^2}{2}\frac{\Omega^2}{2\,K_x^2}+\frac{\chi_{13}^4}{24}\frac{\Omega^4}{K_x^4}\right)}. \tag{22}$$

The exact and asymptotic Green's functions are compared in the third region in Fig.4.

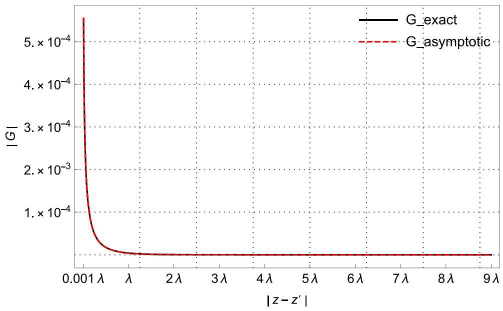


**Figure 4**. Comparison of exact and asymptotic Green's functions for a three layered media for the third region

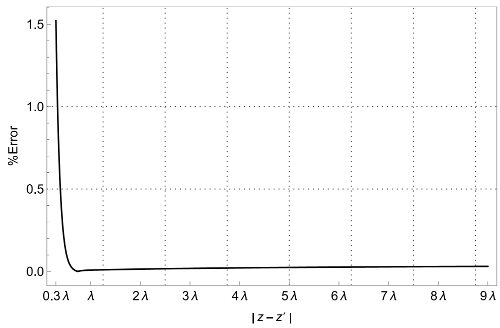


**Figure 5.** Relative error of exact and asymptotic Green's function for a three-layered media for the third region

As seen in Figure 5, the error stays the same for all distances between the source and the measuring point.

## 2.2. Parametric Analysis For a 3-Layered Media

The order of magnitude of the ratios of the layer velocities allows us to use parametric analysis in asymptotic expansions of the coefficient of Green's function given by Eqn. (18) and (22) in the first and third regions, respectively. By applying parametric analysis, the smallness of nondimensional quantities $\chi_{mn}$ $(m, n = 1,2,3)$ permit certain terms to be eliminated in the asymptotic expansion of coefficient and it enables the speed of calculations within acceptable accuracy.

For the first region, let us take the configuration where the velocities are in increasing order of magnitude, that is, $c_3 \ll c_2 \ll c_1$ . In this case, the term $^1/_{\chi_{13}}$ $(^1/_{\chi_{13}} = \ll 1)$, is the smallest term among the terms given in Eqn. (15) and (16). If we neglect the smallest terms in the coefficient $R_3$ which is given by Eqn. (15) and (16), we write the shortened asymptotic coefficient as

$$R_{shortened}^{(I)} = \frac{-i\rho_{13}\chi_{13}\Omega^5\frac{\chi_{12}^4}{2} - i\Omega^5\frac{\chi_{12}^4}{2} + \frac{K_x^2}{\Omega^2}\left(i\rho_{13}\chi_{13}\Omega^5\left(\chi_{12}^2-\frac{1}{\Omega^2}-\frac{\chi_{12}^2}{2\Omega^2}\right)+i\Omega^5\left(\frac{\chi_{12}^2}{4}+\frac{\chi_{12}^4}{4}-\frac{1}{\Omega^2}-\frac{\chi_{12}^2}{2\Omega^2}\right)\right)}{i\rho_{13}\chi_{13}\Omega^5\frac{\chi_{12}^4}{2} - i\Omega^5\frac{\chi_{12}^4}{2} + \frac{K_x^2}{\Omega^2}\left(i\rho_{13}\chi_{13}\Omega^5\left(\chi_{12}^2-\frac{1}{\Omega^2}-\frac{\chi_{12}^2}{2\Omega^2}\right)+i\Omega^5\left(\frac{\chi_{12}^2}{4}+\frac{\chi_{12}^4}{4}-\frac{1}{\Omega^2}-\frac{\chi_{12}^2}{2\Omega^2}\right)\right)}. \quad (23)$$

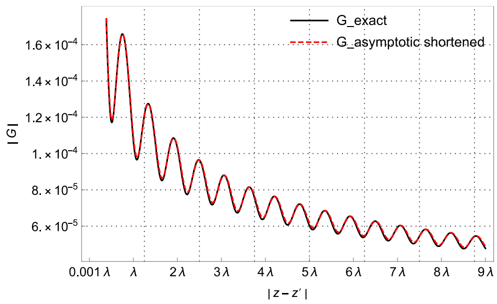


**Figure 6.** Comparison of exact and asymptotic shortened Green's functions for a three layered media for the first region.

In Figure 6, the absolute values of exact Green's function and the asymptotic shortened form of Green's function is compared in terms of distance $|z - z'|$. In this calculation, acoustical and physical parameters are taken as the same numerical values above, except for the sound velocities. Sound velocities are taken as $c_1 = 1600\ m/sec$ , $c_2 = 1000\ m/sec$ , $c_3 = 500\ m/sec$. Thus the ratio of velocities $^1/_{\chi_{13}} =$ 0.3 and there is a significant coincidence between the functions as is depicted in Figure 6.

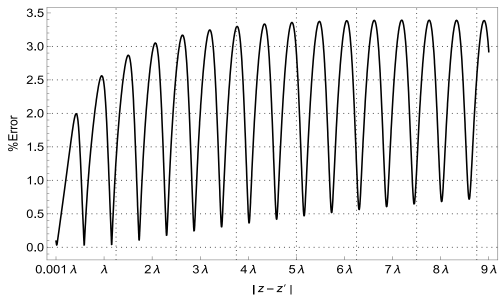


**Figure 7**. Relative error of exact and asymptotic shortened Green's function for the first region.

The graph of the relative error between exact and asymptotic shortened Green's functions is shown in Figure7 which is bounded by 3.5 % for all distance ranges. For the third region, the order of velocities is considered as $c_1 \ll c_2 \ll c_3$ where $c_1 = 500\ m/sec$ , $c_2 = 700\ m/sec$ , $c_3 = 1400\ m/sec$. In this case, the term $\chi_{13} = c_1/c_3 \ll 1$ is the smallest term. Then, the terms $\chi_{13}$ are neglected in the coefficient $R_3^{(III)}$ expressed by eqn (22), and asymptotic shortened Green's function's coefficient is obtain as

$$R_{shortened}^{(III)} = \frac{\left(1 - \frac{\Omega^2}{2\,K_x^2} + \frac{1}{24}\frac{\Omega^4}{K_x^4}\right) - \rho_{13}}{\left(1 - \frac{\Omega^2}{2\,K_x^2} + \frac{1}{24}\frac{\Omega^4}{K_x^4}\right) + \rho_{13}} \quad (24)$$

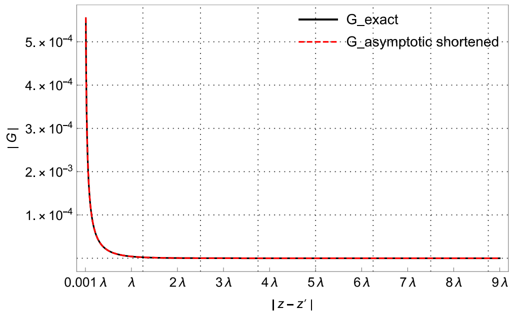


**Figure 8.** Comparison of exact and asymptotic shortened Green's functions for a three-layered media for the third region.

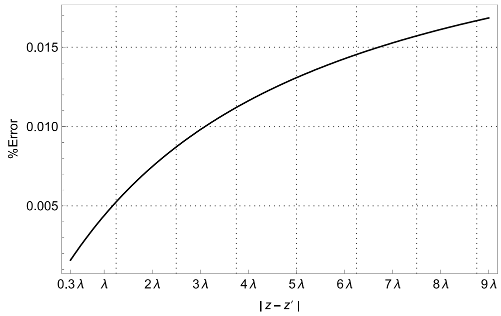


**Figure 9.** Relative error of exact and asymptotic shortened Green's function for a three-layered media for the third region.

It can be seen from Figures 8 and 9 that the compatibility between exact and asymptotic shortened Green's functions is quite favorable in the third region.

**Table 1.** CPU time in seconds per point for distance $|z - z'| = 3\lambda$ for exact Green's, asymptotic Green's and asymptotic shortened Green's function in the first region for 3-layered media.

| Ratio of velocities | Exact Green's Function | Asymptotic Green's Function | Asymptotic Shortened Green's Function |
|---|---|---|---|
| $1/\chi_{13} = 0.3$ | 0,000501383 | 0,000457215 | 0,000456886 |

Therefore, we can say that the computation times are very close in this region. Hence, the analysis of the computational times is done only in the first region by Table 1. It is clearly observed that the CPU times decrease in case of asymptotic and asymptotic shortened form of Green's functions which proves to be an important advantage in imaging algorithms where the Green's function is required to be computed recursively.

## 3. 4-LAYERED MEDIA

For a 4-layered media, the geometry of problem is given in the following figure.

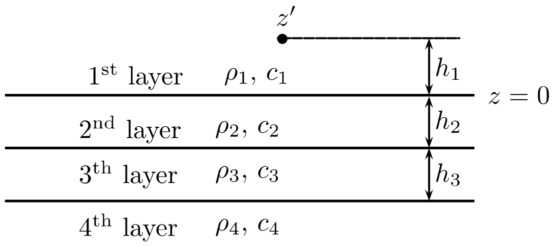


**Figure 11.** Geometry of 4-layered media.

$r = (x', z')$ and $r = (x, z)$ represent source and measurement locations, $c_1$ , $c_2$, $c_3$ and $c_4$ are acoustic wave speeds, and $\rho_1$, $\rho_2$, $\rho_3$ and $\rho_4$ are densites of layers 1, 2, 3 and 4, respectively. The coefficient appearing in equation (1), in this setting, is given by

$$R_4 = \frac{E_4}{\Delta_4} \tag{25}$$

where

$$\begin{aligned} E_4 = {} & K_{z_1} coshK_{z_2} \Big\{K_{z_3} cosh\left(K_{z_3}(1-h_{32})\right)\left(K_{z_1} - \rho_{14}K_{z_4}\right) \\ & + sinh\left(K_{z_3}(1-h_{32})\right)\left(\rho_{34}K_{z_1}K_{z_4} - \rho_{13}K_{z_3}^2\right)\Big\} \\ & + sinhK_{z_2}\Big\{K_{z_3} cosh\left((1-h_{32})K_{z_3}\right)\left(\rho_{12}K_{z_2}^2 - \rho_{24}K_{z_1}K_{z_4}\right) \\ & + sinh\left((1-h_{32})K_{z_3}\right)\left(K_{z_2}^2 K_{z_4}\rho_{12}\rho_{34} - \rho_{23}K_{z_1}K_{z_3}^2\right)\Big\} \end{aligned} \tag{26}$$

and

$$\begin{aligned} \Delta_4 = {} & K_{z_2} coshK_{z_2} \Big\{K_{z_3} cosh\left(K_{z_3}(1-h_{32})\right)\left(K_{z_1} + \rho_{14}K_{z_4}\right) \\ & + sinh\left(K_{z_3}(1-h_{32})\right)\left(\rho_{34}K_{z_1}K_{z_4} + \rho_{13}K_{z_3}^2\right)\Big\} \\ & + sinhK_{z_2}\Big\{K_{z_3} cosh\left((1-h_{32})K_{z_3}\right)\left(\rho_{12}K_{z_2}^2 + \rho_{24}K_{z_1}K_{z_4}\right) \\ & + sinh\left((1-h_{32})K_{z_3}\right)\left(K_{z_2}^2 K_{z_4}\rho_{12}\rho_{34} + \rho_{23}K_{z_1}K_{z_3}^2\right)\Big\}. \end{aligned} \tag{27}$$

Similar to $R_3$, the coefficient $R_4$ can also be written as a piecewise function for the first, second and third regions of integration, as $K_x < \Omega$, $\Omega - \varepsilon < K_x < \Omega + \varepsilon$ and $K_x > \Omega$ , respectively and the coefficient of layered Green's function is written as

$$R_4 = \begin{cases} R_4^{(I)}, & K_x < \Omega \\ R_4^{(II)}, & K_x \in (\Omega - \varepsilon, \Omega + \varepsilon) \\ R_4^{(III)}, & \Omega < K_x. \end{cases} \tag{28}$$

In the 4-layered media, we take into account the leading terms of series expansion of sinh and cosh functions appearing in the numerator and denominator in Eqn. (26)-(27) as follows:

$$coshK_{z_i} \sim 1 \text{ and } sinhK_{z_i} \sim K_{z_i} \tag{29}$$

Unlike layer 3, performing the asymptotic expansion of the coefficient in layer 4, we take the first terms of the expansions of the hyperbolic functions in (26)-(27) and the first 3 terms of the expansions of the wave numbers defined in terms of square root functions in the first and third integration regions, respectively. We analyze it in two cases.

**Case 1**

According to the order of the variable of frequency, the coefficient of Green's function can be written in the first region briefly as

$$R_4^{(I)} = \frac{c_1\Omega + c_2\Omega^2 + (1-h_{32})c_3\Omega^2 + (1-h_{32})c_4\Omega^3}{d_1\Omega + d_2\Omega^2 + (1-h_{32})d_3\Omega^2 + (1-h_{32})d_3\Omega^3} \quad (30)$$

where the constants $c_1, c_2, c_3, c_4$ and $d_1, d_2, d_3, d_4$ can be easily determined from equations (26) and (27) which are given by eqns. (A1) and (A2) in appendix A.

For $\Omega \gg 1$, equation (30) takes the form

$$R_4^{(I)} \sim \frac{c_4 + (c_2 + c_3)\frac{1}{\Omega}}{d_4 + (d_2 + d_3)\frac{1}{\Omega}} \quad (31)$$

We then can express equation (31) asymptotically as

$$R_4^{(I)} \sim \frac{1}{d_4}\left(c_4 + \left(\frac{(c_2 + c_3)1}{\Omega}\right)\right)\left(1 - \left(\frac{d_2 + d_3}{d_4}\right)\frac{1}{\Omega}\right) + \frac{c_4}{d_4}\left(\frac{d_2 + d_3}{d_4}\right)^2\left(\frac{1}{\Omega}\right)^2 \quad (32)$$

Here, the coefficients $c_i$ and $d_i$ include the square root functions. When expanding the asymptotic series of root functions, terms of order up to six $\left(\frac{K_x^6}{\Omega^6}\right)$ should be kept to reduce the relative error between the exact coefficient of the Green's function and its asymptotic expression. The asymptotic expansion of coefficient is given by eqn. (A3) presented in appendix A.

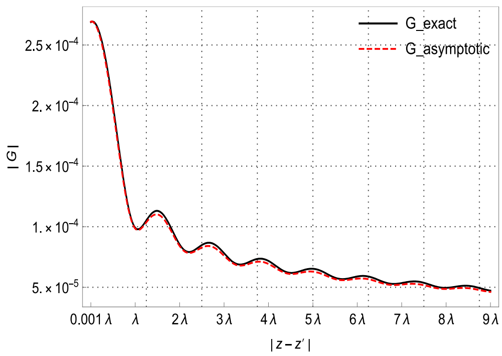


**Figure 12.** Comparison of exact and asymptotic shortened Green's functions for a four layered media for the first region.

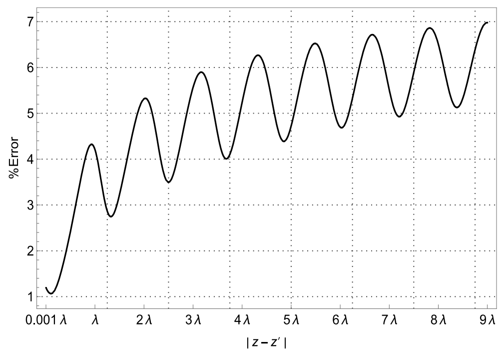


**Figure 13.** Relative error of exact and asymptotic shortened Green's function for a three-layered media for the first region.

Figures 12 and 13 illustrate that the exact and asymptotic Green's functions match quite well in the first region demonstrating the validity of the considered approach.

**Case 2:**

The calculation performed above for $R_4$ in the first region can be similarly repeated for the third region. It is clear that the term $\frac{\Omega}{K_x}$ should be taken as the small parameter in this region. Since this region is semi-infinite, it will be sufficient to expand the square root function up to 4th-order. For $\Omega \ll K_x$, we have

$$R_4^{(III)} \sim \frac{1}{d_4}\left(c_4 + \frac{c_2 + c_3}{K_x}\right)\left(1 - \frac{d_2 + d_3}{d_4}\right)\frac{1}{K_x} + \frac{c_4}{d_4}\left(\frac{d_2 + d_3}{d_4}\right)^2 \frac{1}{K_x^2} \qquad (33)$$

which is given explicitly in appendix A by eqn. (A4).

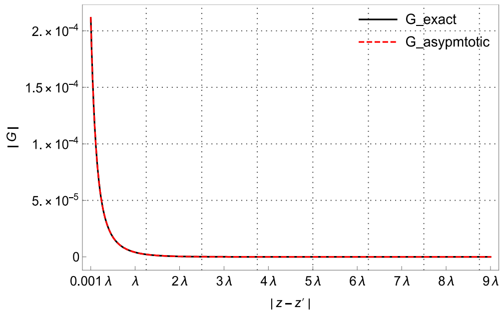


**Figure 14.** Comparison of exact and asymptotic shortened Green's functions for a four layered media for the third region.

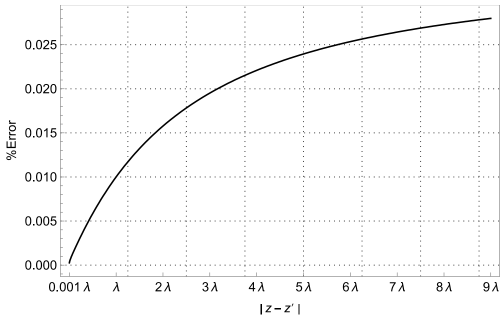


**Figure 15.** Relative error of exact and asymptotic shortened Green's function for a four-layeredmedia for the third region.

Figure 14 demonstrates the numerical comparison with the exact and asymptotic shortened Green's functions while Figure 15 shows the relative error between the exact and asymptotic shortened Green's functions for four layered media for the third region.

**Table 2.**CPU time in seconds per point for distance $|z - z'| = 3\lambda$ for exact Green's and asymptotic Green's function in the first region for 4 layered media.

| **Exact Green's Function** | **Asymptotic Green's Function** |
|---|---|
| 0,00007509 | 0,00003565 |

It is seen that from Table 2 the computation time of the asymptotic Green's function is quite short.

## 5. CONCLUSION

Asymptotic series expansions for the reflection coefficient ($R_n$) of the component of the acoustic Green's function obtained for the 3- and 4-layer geometry, see eqns. (18), (22), (32) and (33), with the source and the observation points in the first region, are performed by dividing the integration region according to the temporal frequency ($\Omega$) and spatial frequency ($K_x$). Since the terms of the coefficients are written as polynomials on expanding the asymptotic series with respect to the regions containing the acoustic velocities of the layers, a parametric analysis is performed according to the ratios of the acoustic velocities. Green's functions written in polynomial form over the regions are analyzed and the leading terms are retained, and the next order terms (the lowest order term) are neglected. The relative errors between the exact Green's function and the Green's functions analyzed parametrically according to the velocities are calculated. It is observed that, the parametrically and asymptotically analyzed Green's functions in the layered structure agree quite well with the exact ones and their relative errors are in acceptable range. Calculation time comparisons are also carried out between Green's function given in the shortened form and the full Green's function for layered structures by asymptotic and parametric analysis. From Table 1 and Table 2, it can be seen that the reduced computation time of asymptotic and shortened asymptotic Green's functions will save time in photoacoustic imaging algorithms particularly due to recursive calculations required by the Green's functions.

## ACKNOWLEDGEMENTS

This work was supported by TUBITAK of Turkey through the ARDEB-1001 Program under Grant No. 119E624.

## CONFLICT OF INTEREST

The authors stated that there are no conflicts of interest regarding the publication of this article.

## AUTHORSHIP CONTRIBUTIONS

Autors' contributions are equal.

## REFERENCES

[1] Uzun B, Yücel H. An inverse source problem connected with thermoacoustic imaging in multi-layer planar medium. Journal of Mathematical Imaging and Vision 61 (2019): 874-884

[2] Xu M, Wang LV. Universal back-projection algorithm for photoacoustic computed tomography. Physical Review E, 2005; 71(1), 016706.

[3] Schoonover RW, Anastasio MA. Image reconstruction in photoacoustic tomography involving layered acoustic media. JOSA A, 2011; 28(6), 1114-1120.

[4] DiNapoli FR, Deavenport RL. Theoretical and numerical Green's function field solution in a plane multilayered medium. The Journal of the Acoustical Society of America, 1980; *67*(1), 92-105.

[5] Dural G, Aksun MI. Closed-form Green's functions for general sources and stratified media. IEEE transactions on microwave theory and techniques, 1995;43(7), 1545-1552.

[6] Kaplunov J, Prikazchikov D, Sergushova O. Multi-parametric analysis of the lowest natural frequencies of strongly inhomogeneous elastic rods. Journal of Sound and Vibration, 2016; 366, 264-276.

[7] Kaplunov YD, Prikazchikova LAE. Low-frequency vibration modes of strongly inhomogeneous elastic laminates. Известия Саратовского университета. Новая серия. Серия: Математика. Механика. Информатика, 2018; 18(4), 447-457.

[8] Özdemir Ö, Yücel H, Uçar YE, Erbaş B, Ege N. Green's functions for a layered high-contrast acoustic media. The Journal of the Acoustical Society of America, 2022; 151(6), 3676-3684.

[9] Prikazchikova L, Aydın YE, Erbaş B, Kaplunov J. Asymptotic analysis of an anti-plane dynamic problem for a three-layered strongly inhomogeneous laminate. Mathematics and Mechanics of Solids, 2020; 25(1), 3-16.


**APPENDIX A**

$$
\begin{gathered}
c_1 = K_{z_1} - \rho_{14} K_{z_4}, \\
c_2 = \rho_{12} K_{z_2}^2 - \rho_{24} K_{z_1} K_{z_4}, \\
c_3 = \rho_{34} K_{z_1} K_{z_4} - \rho_{13} K_{z_3}^2, \\
c_4 = K_{z_2}^2 K_{z_4} \rho_{12} \rho_{34} - \rho_{23} K_{z_1} K_{z_3}^2,
\end{gathered} \tag{A1}
$$

$$
\begin{gathered}
d_1 = K_{z_1} + \rho_{14} K_{z_4}, \\
d_2 = \rho_{12} K_{z_2}^2 + \rho_{24} K_{z_1} K_{z_4,} \\
d_3 = \rho_{34} K_{z_1} K_{z_4} + \rho_{13} K_{z_3,}^2 \\
d_4 = K_{z_2}^2 K_{z_4} \rho_{12} \rho_{34} + \rho_{23} K_{z_1} K_{z_3}^2 \ .
\end{gathered} \tag{A2}
$$

$$
\begin{aligned}
& R_4^{(I)} \sim \Big( 8\chi_4^3 \big( -\chi_4(-1 + h_{32} + \rho_{23})\rho_{34} - (-1 + h_{32})\chi_3^2(\rho_{13} + i\rho_{23}\Omega) + \chi_2^2\rho_{12}(-1 - \\
& i(-1 + h_{32})\chi_4\rho_{34}\Omega) \big) + 4\,\mho^2\chi_4^2 \big( \chi_4^2\rho_{34}(-1 + h_{32} + \rho_{23} - 2i\rho_{12}\Omega + 2\mathrm{i}h_{32}\rho_{12}\Omega) + \\
& \rho_{34}(-1 + h_{32} + \rho_{23} - i\chi_2^2\rho_{12}\Omega + \mathrm{i}h_{32}\chi_2^2\rho_{12}\Omega) + \chi_4 \big( 2\rho_{12} + (-1 + h_{32})(2\rho_{23} + \\
& i(2 + \chi_3^2)\rho_{23}\Omega) \big) \big) + \mho^4 \big( i(-1 + h_{32})(-4 + \chi_3^2)\chi_4^3\rho_{23}\Omega + \rho_{34} \big( -1 - \rho_{23} - \chi_4^4(1 + \\
& \rho_{23}) - i\chi_2^2\rho_{12}\Omega + 2\chi_4^2(1 + \rho_{23} + 2i\rho_{12}\Omega) + h_{32} \big( 1 + \chi_4^4 + i\chi_2^2\rho_{12}\Omega + \chi_4^2(-2 - \\
& 4i\rho_{12}\Omega) \big) \big) \big) \Big) \Big( \Big( 8\chi_4^3 \big( \chi_4(-1 + h_{32} + \rho_{23})\rho_{34} - (-1 + h_{32})\chi_3^2(\rho_{13} + i\rho_{23}\Omega) + \\
& \chi_2^2\rho_{12}(i + (-1 + h_{32})\chi_4\rho_{34}\Omega) \big) + 4\,\mho^2\chi_4^2 \big( -\chi_4^2\rho_{34}(-1 + h_{32} + \rho_{23} - 2i\rho_{12}\Omega + \\
& 2\mathrm{i}h_{32}\rho_{12}\Omega) - \rho_{34}(-1 + h_{32} + \rho_{23} - i\chi_2^2\rho_{12}\Omega + \mathrm{i}h_{32}\chi_2^2\rho_{12}\Omega) + \chi_4 \big( 2\rho_{12} + (-1 + \\
& h_{32})(2\rho_{23} + i(2 + \chi_3^2)\rho_{23}\Omega) \big) \big) + \mho^4 \big( i(-1 + h_{32})(-4 + \chi_3^2)\chi_4^3\rho_{23}\Omega + \rho_{34} \big( 1 - \rho_{23} - \\
& \chi_4^4(1 + \rho_{23}) - i\chi_2^2\rho_{12}\Omega + 2\chi_4^2(-2 + 2\rho_{23} + 2i\chi_2^2\rho_{12}\Omega) + h_{32} \big( -1 + \chi_4^4 + i\chi_2^2\rho_{12}\Omega + \\
& \chi_4^2(2 - 2i\chi_2^2\rho_{12}\Omega) \big) \big) \big) \Big) \Big) \Big/ \Big( (-1 + h_{32})^2 \big( -8\chi_4^3(\chi_3^2\rho_{23} + \chi_2^2\chi_4\rho_{12}\rho_{34}) + \mho^4 \big( (-4 +
\end{aligned} \tag{A3}
$$

$\chi_3^2\,)\chi_4^3\rho_{23}+\chi_2^2\rho_{12}\rho_{34}-4\chi_4^2\rho_{12}\rho_{34}\Big)+4\mho^4\chi_4^2\left(\left((2+\chi_3^2)\chi_4\rho_{23}+\chi_2^2\rho_{12}\rho_{34}+\right.\right.$
$\left.\left.2\chi_4^2\rho_{12}\rho_{34}\right)\Big)^2\,\Omega^2\right)\Bigg)\;\;,\;\mho^2=\frac{\mathrm{K}^2}{\Omega^2}.$

$$R_4^{(III)}\sim((-4(1+(-1+h_{32})\rho_{13}-K\rho_{23}-\rho_{24}+\rho_{34}-h_{32}\rho_{34}+K\rho_{12}\rho_{34})+ 2\frac{\Omega^2}{K^2}\Bigg(-K\rho_{23}+\kappa_3^2\big((-1+h_{32})\rho_{13}-K\rho_{23}\big)-\rho_{24}-\kappa_4^2\rho_{24}+\rho_{34}-h_{32}\rho_{34}+\kappa_4^2\rho_{34}- h_{32}\kappa_4^2\rho_{34}+K\,\kappa_4^2\rho_{12}\rho_{34}+2\,\kappa_2^2(\rho_{12}+K\rho_{12}\rho_{34})+\frac{\Omega^4}{K^4}\Big(\kappa_4^2(\rho_{24}+(-1+h_{32})\rho_{34})+ 2K(\kappa_3^2\rho_{23}-\kappa_2^2\kappa_4^2\rho_{12}\rho_{34})\Big)\Bigg)\Bigg(-\frac{2\Omega^2}{K^2}\Big(-K\rho_{23}+h_{32}K\rho_{23}-2(-1+h_{32})\kappa_3^2(\rho_{13}-K\rho_{23})- \rho_{24}-\kappa_4^2\rho_{24}+\rho_{23}-h_{32}\rho_{34}+\kappa_4^2\rho_{34}-h_{32}\kappa_4^2\rho_{34}-K\kappa_4^2\rho_{34}\rho_{12}+h_{32}K\kappa_4^2\rho_{12}\rho_{34}+ 2\kappa_2^2\rho_{12}(-1+(-1+h_{32})K\rho_{34})\Big)-4\Bigg(+\big(-1+h_{32}\rho_{13}+\rho_{24}-\rho_{34}+h_{32}\rho_{34}-(-1+ h_{32})K(\rho_{23}+\rho_{12}\rho_{34})\big)+\frac{\Omega^4}{K^4}\Big(-\kappa_4^2(\rho_{24}+(-1+h_{32})\rho_{34})+2(-1+h_{32})K(\kappa_3^2\rho_{23}+ \kappa_2^2\kappa_4^2\rho_{12}\rho_{34})\Big)\Bigg)\Bigg)/(4(-1+h_{32})^2K^2\Bigg(\Big(-2+\frac{\Omega^2}{K^2}\Big)\Big(-1+\frac{\Omega^2}{K^2}\kappa_3^2\Big)\rho_{23}+\Big(-1+ \frac{\Omega^2}{K^2}\kappa_2^2\Big)\Big(-2+\frac{\Omega^2}{K^2}\kappa_4^2\Big)\rho_{12}\rho_{34}\Bigg)^2)\,. \tag{A4}$$